Characterisation of timber joists-masonry connections in double-leaf cavity walls – Part 1 Experimental results

Arslan, O.; Messali, F.; Smyrou, E.; Bal, E.; Rots, J. G.

DOI
10.1016/j.istruc.2024.107164

Publication date
2024

Document Version
Final published version

Published in
Structures

Structures 68 (2024) 107164

Contents lists available at ScienceDirect

Structures

journal homepage: www.elsevier.com/locate/structures

Characterisation of timber joists-masonry connections in double-leaf cavity walls – Part 1: Experimental results

O. Arslan [a,b,*], F. Messali [a], E. Smyrou [b], İ.E. Bal [b], J.G. Rots [a]

[a] Faculty of Civil Engineering and Geosciences, Delft University of Technology, Delft, the Netherlands,
[b] Research Centre for Built Environment NoorderRuimte, Hanze University of Applied Sciences, Groningen, the Netherlands

ARTICLE INFO

Keywords:
Unreinforced masonry
As-built condition
Strengthened condition
Timber joists
Cavity walls
Connections
Wall ties
Helical Bars

ABSTRACT

Post-earthquake structural damage shows that out-of-plane (OOP) wall collapse is one of the most common failure mechanisms in unreinforced masonry (URM) buildings. This issue is particularly critical in Groningen, a province located in the northern part of the Netherlands, where low-intensity induced earthquakes have become an uprising problem in recent years. The majority of buildings in this area are constructed using URM and were not designed to withstand earthquakes, as the area had never been affected by tectonic seismic activity before. OOP failure in URM structures often stems from poor connections between structural elements, resulting in insufficient restraint to the URM walls. Therefore, investigating the mechanical behaviour of these connections is of prime importance for mitigating damages and collapses in URM structures.

This paper presents the results of an experimental campaign conducted on timber joist-masonry cavity wall connections. The specimens consisted of timber joists pocketed into masonry wallets. The campaign aimed at providing a better understanding and characterisation of the cyclic axial behaviour of these connections. Both as-built and strengthened conditions were considered, with different variations, including two tie distributions, two pre-compression levels, two different as-built connections, and one strengthening solution. The experimental findings underscored that incorporating retrofitting bars not only restores the system's initial capacity but also guarantees deformation compatibility between the wall and the joist. This effectively enhances the overall deformation capacity and ductility of the timber joist-cavity wall system.

1. Introduction

Out-of-plane (OOP) wall collapse is one of the most common failure mechanisms in unreinforced masonry (URM) structures. Insufficient or ineffective connections at wall-to-wall, wall-to-floor or wall-to-roof levels are one of the main reasons for OOP failures [1]. This issue is particularly critical in Groningen, a province located in the northern part of the Netherlands, where low-intensity human-induced earthquakes have been occurring since 1991 due to gas extraction. The majority of buildings in this area are constructed using URM and were not designed to withstand earthquakes, as the area had never been affected by tectonic seismic activity before. Hence, the assessment of URM buildings in the Groningen province has become of high relevance.

URM buildings in Groningen are typically low-rise, which generally embody vulnerable structural elements such as large openings, slender and cavity walls, and timber diaphragms, and lack any specific seismic detailing, including connections between structural elements. For example, according to a study by Arup [2], traditional Dutch houses with cavity walls and flexible diaphragms make up 23.8 % of the inventory in the Groningen province. Additionally, in common Dutch practice, the timber joist end is either simply placed on a pocket located in the inner leaf of a cavity wall, or a hook anchor is added to improve the connection [3].

Wall-to-floor connections are essential players in ensuring the global stability of URM structures against seismic and other dynamic actions. If these connections are inadequate or absent, an earthquake-resistant box-type behaviour cannot be ensured, and local wall failure mechanisms such as bending, sliding, and out-of-plane wall collapse may occur [4,5]. Traditional wall-to-floor connections in URM structures can be categorised as friction-based (hereinafter referred to as *mortar pocket connections*) and anchor-based. The mortar pocket connection can be characterised as the simplest and oldest construction practice, in which

* Corresponding author at: Faculty of Civil Engineering and Geosciences, Delft University of Technology, Delft, the Netherlands.
E-mail addresses: o.arslan@tudelft.nl, o.arslan@pl.hanze.nl (O. Arslan), F.Messali@tudelft.nl (F. Messali), e.smyrou@pl.hanze.nl (E. Smyrou), i.e.bal@pl.hanze.nl (İ.E. Bal), J.G.Rots@tudelft.nl (J.G. Rots).

https://doi.org/10.1016/j.istruc.2024.107164
Received 29 January 2024; Received in revised form 13 August 2024; Accepted 23 August 2024
Available online 28 August 2024

the joist is inserted over the whole width or half the width of a masonry wall for thin or thick walls, respectively. The anchor-based connections are a relatively modern solution, in which the timber joist is connected to the masonry using connectors, such as iron straps, metal tie-bars or hooked anchors. Joist-masonry connections have been extensively investigated in the literature. The essential research is summarised in the following paragraphs by distinguishing the experimental campaigns conducted at either the building level or component (single connection) level along with some illustrative examples of wall-to-floor connections (Fig. 1).

As stated in the literature, in case of mortar pocket connections, frictional resistance plays an important role in the development of OOP mechanisms of the connected walls [6]. In order to understand the dynamic behaviour of historic stone masonry with timber floors and roofs and evaluate possible strengthening solutions, an experimental campaign on three full-scale two-storey buildings was carried out at the EUCENTRE laboratory in Pavia [7]. One of the tested structures was representative of a vulnerable building lacking anchors between masonry walls and timber floors [8]. The specimen showed a local out-of-plane failure due to the poor connections. In tests of another specimen, named Building 2, the floor diaphragm-to-wall connections were improved by the inclusion of anchors, which allowed to prevent premature OOP failures. Consequently, improving the connections in the building led to a global response, resulting in increased lateral strength and stiffness.

With the aim of characterising the seismic behaviour of typical Dutch houses, an extensive multiscale testing programme was performed at EUCENTRE laboratories [9]. Specifically, this campaign aimed at investigating the seismic behaviour of structural components, assemblies and complete buildings. Among others, full-scale shaking table tests of a cavity wall terraced house [10] and a double-wythe clay-brick detached house [11] with flexible timber diaphragms were conducted. Two different connections: mortar pocket connections and connections with hook anchors, were used between timber joists and masonry walls for both the terraced and detached houses to represent the actual as-built condition. The hook anchors were placed on the pocket of the inner leaf for the cavity wall terraced house, while they were inserted into the masonry between the two wythes for the detached house. It was reported that no sliding or significant differential displacements between joists and masonry were recorded, although the connections were damaged. For this reason, the connections were, in general, assessed to perform adequately. However, since the research focused on the global dynamic behaviour of the buildings, the performance of the single connections was not further investigated.

With regard to tests conducted at the component level and specifically on mortar pocket connections, Almeida et al. [12] performed an experimental study to characterise the frictional resisting mechanism between a timber floor and masonry (Fig. 1a). In this experimental programme, triplet tests were conducted to investigate the cyclic friction of timber-timber and mortar-timber connections. The wall-to-floor connection was designed to be representative of unstrengthened conditions, in which the timber joist was supported by a masonry wall. Two different mortar types were considered: antique mortar and modern mortar. The antique mortar represented a weak-quality mortar used in historic buildings consisting of hydraulic lime and sand, while the modern one was a high-quality mortar without aggregates. They found that the surface roughness of the timber can be a governing factor in increasing friction resistance, while the loading rate had no influence on the friction behaviour. The authors also mentioned that the specimens with antique mortar did not exhibit a frictional type of behaviour and were hence excluded from the experiment since the mortar was grinding, breaking up and degrading into powder.

Lin and Lafave [13] conducted a testing campaign on two different types of typical wall-to-floor connections, with and without nailed strap anchors (Fig. 1f). The specimens were subjected to three different loading methods, namely: static monotonic, static cyclic loading and dynamic cyclic loading. The specimens represented a common typology for joist-wall connections in URM buildings. The as-built mortar pocket

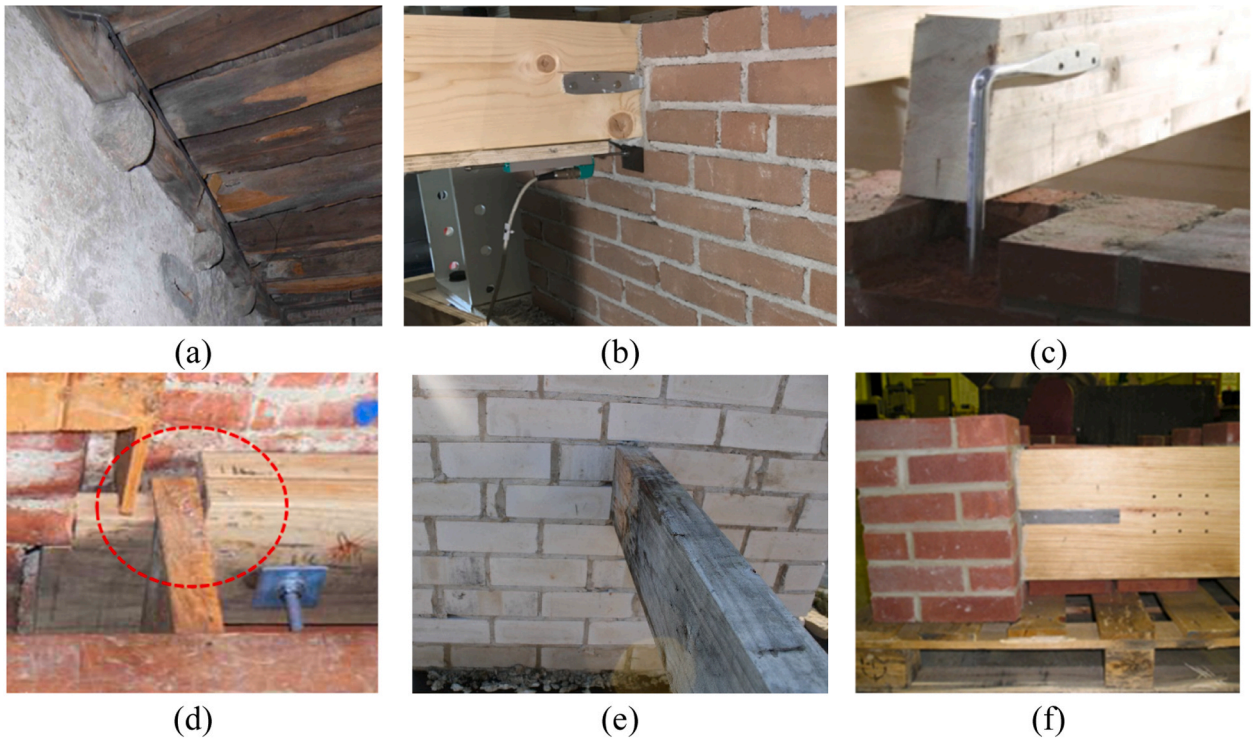

Fig. 1. Examples of wall-to-floor connections: timber floor resting on masonry wall [12] (a), timber joist seated in a pocket with hook anchor [20] (b), hook anchor embedded in the masonry wall [11] (c), wall-to-diaphragm connections with timber blocking [18] (d), joist masonry wall connections with cavity wall tie connections [3] (e), and strap anchor connection [13] (f).

connections provided a lower strength capacity compared to the specimens with nailed strap anchors. An average friction coefficient of 0.5 was defined for the former specimens, in good agreement with the values found in previous literature, e.g. those given in the American Civil Engineer's Handbook [14].

The efforts to reduce the risk of OOP failure focus on improving connections between diaphragms and walls. One of the main retrofitting solutions applied for masonry buildings is through the use of anchorage systems [15]. Porcarelli et al. [16] conducted an experimental campaign to investigate the tension and shear load behaviour of anchors for stone masonry buildings. It was mentioned that the capacity increases under tension load as the anchor embedment depth increases. Regarding the shear behaviour of anchors, Giuriani et al. [17] conducted an experimental investigation to characterise the behaviour of anchors employed to transfer horizontal shear forces between diaphragms and walls. Another study was conducted by Giongo et al. [18] on the performance of the shear transferring connection anchors between timber floors and masonry walls (d). A timber blocking element is used to represent the seismic strengthening of ancient URM buildings. It was observed that the thickness of the blocking element had no impact on the shear behaviour of the specimens.

Mirra et al. [19] conducted an experimental investigation on different timber joist-masonry wall connections in single-wythe calcium silicate masonry walls, representing part of cavity walls in traditional Dutch houses (Fig. 1b). A total of seven configurations were studied, including mortar pocket connections, hook anchors, and strengthened connections. They focused on timber-masonry connections in a single-leaf wall and the absence of an overburden load in the inner leaf.

Timber joists and cavity walls are common construction practices not only in the Netherlands [10] but also elsewhere in the world [21–23]. Although previous studies have already provided insight into the seismic behaviour of wall-to-diaphragm connections, there is a lack of experimental results that consider cavity walls with timber joists in as-built and strengthened conditions representing timber joist-masonry cavity wall connections in typical Dutch masonry structures. Thus, an experimental campaign has been conducted at BuildinG Laboratory of Hanze University of Applied Sciences, which aimed at thoroughly characterising the cyclic axial behaviour of timber-joist connections in as-built conditions as well as to assess the performance of possible strengthening solutions for the Dutch context but also can be extended to other countries worldwide with similar configuration. Section 2 describes the geometry of the specimens, the test setup, and the adopted testing protocol, as well as the companion tests conducted at the material level to identify the material properties. Section 3 presents and discusses the results of the experimental campaign for connections in both unstrengthened and strengthened conditions. Special attention is devoted to the identification of failure modes and hysteretic behaviour for each group of tests performed. Finally, Section 4 summarises the main findings of the experimental campaign and recommends future developments.

2. Specimen characteristics

The experiments presented in this paper aim to provide a comprehensive characterisation of the cyclic axial behaviour of timber joist-cavity wall connections in as-built conditions and to assess the performance of possible strengthening solutions.

2.1. Test specimens

Timber diaphragms (floors or roofs) are commonly used in URM buildings [24]. The timber floor joists are typically connected to the masonry walls by inserting the joists in pockets in the masonry so that the connection mostly relies on a frictional resisting mechanism. As an alternative, in some countries, such as the Netherlands, hook anchors are used to ensure a stronger connection. For this reason, these two alternative constructive solutions are considered for the experimental campaign.

All wallets tested in this study were constructed on a steel beam by an experienced mason to ensure the best possible quality control. Each specimen consisted of a cavity wall with metal ties and a timber joist laid in a pocket in the inner leaf of the wall. The specimens were left to cure for at least 28 days prior to testing (as-built conditions) or to applying the retrofitting solutions (strengthened conditions).

Six wallets were tested in unstrengthened connections, reproducing cavity walls with timber joists in as-built conditions. A statistical analysis conducted by the authors [3] shows that cavity walls in Dutch construction practice are often composed of an inner load-bearing leaf made of calcium silicate brick masonry (CS), an outer non-load-bearing leaf made of clay brick masonry (CB) and a cavity (Fig. 2a). Full-size bricks were used in the experimental campaign, including the CS brick, which had a size of roughly 210×70×102 mm, and the CB brick, which was roughly 210×50×100 mm. In the specimens, the inner leaf was nominally 1030 mm high, 930 mm wide, and 102 mm thick, while the outer leaf was approximately 950 mm high, 930 mm wide and 100 mm thick.

The timber joist, with a size of 55 × 155 mm and a total length of 1600 mm long, was inserted in a pocket of the inner leaf, with a 10-mm-thick mortar bed-joint below and above the joist. It should be noticed that embedding the timber joist in mortar bed joints is a common practice not only in the Netherlands [10,25] but also elsewhere around the world [26]. The timber joists used in this experimental campaign were chosen to be in good condition to eliminate the uncertainties that may stem from wood decay. Wood decay can be found in old buildings with timber floors under conditions of high wood moisture content [27–29]. It should be noted that the friction coefficient in the case of wood decay in timber joists may differ from that found in this study due to imperfections on the contact surface. Table 1 summarises the characteristics of the tested walls, which are described in detail in the following paragraphs, grouped per typology of the test.

Regarding the as-built wall-to-wall connections, L-shaped ties with a diameter of 3.6 mm and a total length of 200 mm were embedded between two bricks in the mortar joint. The geometry and characteristics of the ties were selected consistently to those used in a previous testing campaign conducted by the authors [30]. The embedment length differed at each end of the tie: the zigzag end was embedded in the outer leaf of the cavity wall for a length of 50 mm, whereas the hooked ends were embedded in the inner leaf of the cavity wall for a length of 70 mm.

Regarding the as-built wall-diaphragm connections, the timber joist end is either simply placed on a pocket located in the inner leaf of a cavity wall, an as-built mortar pocket connection, or a 14-mm-diameter hook anchor is added to improve the connection. Both solutions are consistent with the construction practice in the Netherlands. For the latter solution, the connection is provided by the hook anchor, fastened to the timber joist with three screws. In the experimental campaign, the hook anchor was passed through the CS leaf, bearing against the exterior surface of the CS leaf. The details of the cavity wall tie and hook anchor are displayed in Fig. 2.

Two different levels of pre-compression were applied on top of the load-bearing calcium-silicate leaf, namely 0.1 MPa and 0.3 MPa. Meanwhile, the non-load-bearing clay leaf functioned as a free-standing cantilever wall, following common construction practices in the Netherlands. The applied pre-compression levels were considered to be representative of a cavity wall at the first and second levels of a typical URM residential building [31].

After completing the testing of the specimens in as-built condition, the six walls (J1, J2, J3, J4, J5 and J6) were retrofitted by connecting the outer leaf and the timber joist with helical bars and retested. The helical bar is a twisted stainless steel reinforcing bar. Two helical bars with a diameter of 6 mm and a total length of 335 mm were used. The retested specimens were named by adding "T" onto the front of the names of the corresponding as-built specimens, i.e., TJ1 to TJ6 (Table 1).

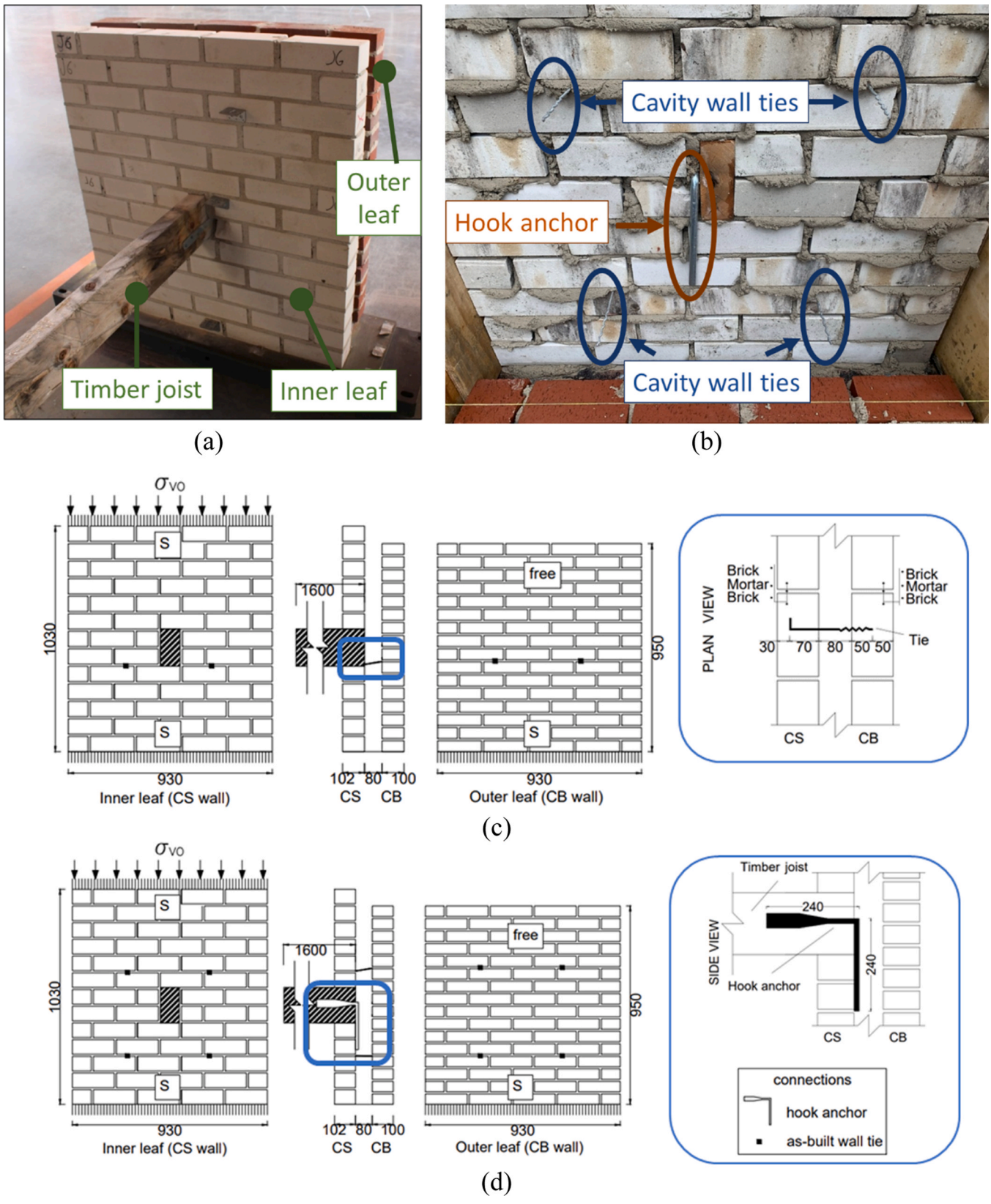

Fig. 2. Geometry of the tested wallets and construction details: view of the cavity wall specimen with timber joist (a), view of the external side of the inner leaf of a cavity wall (b), the geometry of a specimen with two as-built cavity wall ties and details of cavity wall tie connection (c) and the geometry of a specimen with four as-built cavity wall ties and details of hook anchor connection (d) (dimensions are in mm). Note that S is simply-supported edge and Free is free edge.

Table 1
Overview of the specimens in terms of applied pre-compression level and connections details in unstrengthened and strengthened conditions.

Specimen Type	Specimen Name	Initial pre-comp. level	As-built condition		Strengthened condition
			Timber joist-wall connection	Number of As-built wall ties	Timber joist-wall connection
Unstrengthened connections	J1	0.1	Pocket connection	2 ties	-
	J2	0.1	Hook anchor	2 ties	-
	J3	0.1	Pocket connection	4 ties	-
	J4	0.1	Hook anchor	4 ties	-
	J5	0.3	Pocket connection	4 ties	-
	J6	0.3	Hook anchor	4 ties	-
Connections with strengthened helical bars	TJ1*	0.1	Pocket connection	2 ties	Helical bar
	TJ2*	0.1	Hook anchor	2 ties	Helical bar
	TJ3*	0.1	Pocket connection	4 ties	Helical bar
	TJ4*	0.1	Hook anchor	4 ties	Helical bar
	TJ5*	0.3	Pocket connection	4 ties	Helical bar
	TJ6*	0.3	Hook anchor	4 ties	Helical bar

* After testing in the as-built condition, the specimens were strengthened and retested.

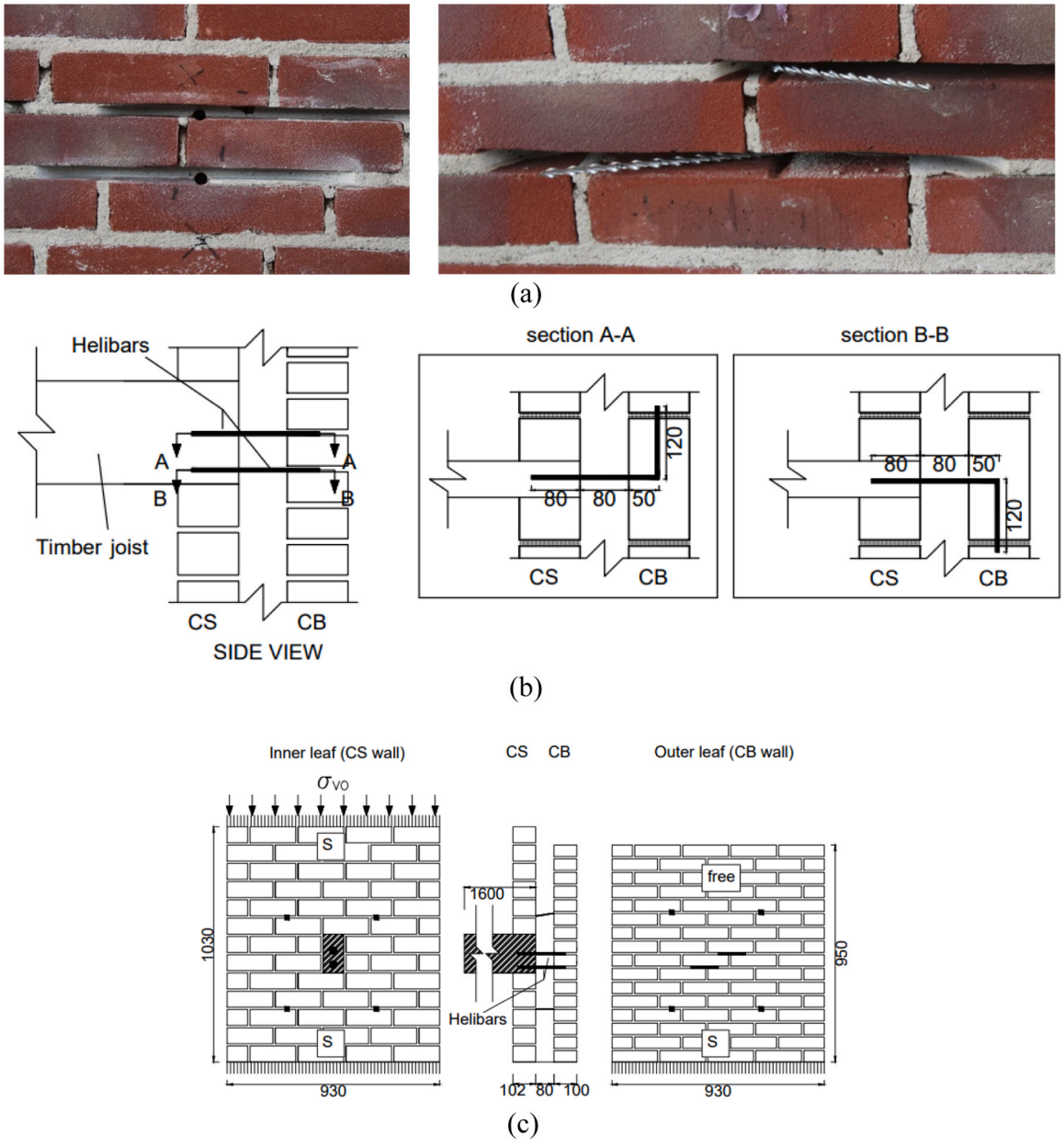

Fig. 3. Details of the strengthened connections with helical bars: installing procedure for helical bars (a), schematic overview of helical bars (b), and test wall configuration for the strengthened connection (c) (dimensions are in mm).

To simulate the real installation of helical bars, two holes perpendicular to the wall and in the orientation of the joist were drilled through the whole thickness of the outer leaf and 80 mm through the joist (Fig. 3a). Then, the clay mortar bed was cut with a minimum length of 120 mm for each helical bar. First, the spiral bars were installed through the predrilled holes to connect the veneer to the joist. After installing helical bars in the uniaxial direction of the joist, the spiral bars were bent 90 degrees in the bed joint of the outer veneer with approximately a length of 120 mm. Therefore, out of a total length of 335 mm, a length of 80 mm was embedded in the joist, 80 mm of the bar was in the cavity gap, an additional length of 50 mm was embedded in the outer leaf for half of its thickness, while the rest of the tie (which was around 120 mm) was bent and embedded in the bed-joint of the clay leaf (Fig. 3b). Finally, the slots were filled with high-strength epoxy materials.

2.2. Test Setup and the boundary conditions

The test setup was composed of a stiff reaction frame, two air bellows and an electro-mechanic actuator. In order to restrain the specimen to the frame, a bottom steel plate was used. A timber plywood plate was attached to the bottom steel beam to provide proper adhesion for the specimens. The specimens were built on the steel beam, while high-adjustable steel support was used during the construction period to support the timber joist. The support was removed when the specimen was placed in the test setup. After that, the bottom steel plate was bolted to the two carriers on the legs of the frame.

The specimens were loaded via the joist with an electric actuator, which had a capacity of 30 kN for both positive (pulling) and negative (pushing) directions, integrated with a data acquisition system. The actuator was aligned horizontally along the centreline axis of the joist. The free end of the joist was connected to the actuator, allowing for the transfer of the applied load in the uniaxial direction of the joist through the pressure apparatus. It should be noted that due to the way the joist was connected to the actuator, rotations and vertical displacements of the end of the joist were prevented.

The specimens were subjected to vertical pre-compression via two air bellows to simulate the effect of load-bearing walls acting on the inner leaf of the masonry structure. A steel plate was placed on the top of the load-bearing inner leaf in order to distribute the pre-compression stress uniformly at every point. In order to prevent OOP movement of the top end of the inner leaf of the cavity wall, a pair of steel braces was added to the test setup. The braces were fixed on one end of the test setup and on the other to the top of the inner leaf. The details of the application of the pre-compression and of the steel braces are shown in Fig. 4. A vertical dead load of 100 kg was applied to the middle of the joist to simulate the self-weight of the portion of the floor supported by the joist.

The top horizontal edge of the inner leaf was restrained against vertical translation due to the presence of the air bellows. Because of that, in the case of overturning and subsequent vertical displacements of the top block of the inner leaf, variations in the vertical pre-compression might have occurred. Hence, the initially applied overburden is called the initial pre-compression level, as in Table 1. The bottom horizontal edge of the inner leaf was bonded to the timber plywood, which provide partial restrain against rotation at the base of the wall. Hence, it can be expected that the resultant of the vertical load will be located in between the wall face and the wall centreline. The first assumption considers hinged conditions, while the second considers clamped conditions at the bottom of the inner leaf. Morandi [32] reported that assuming the ends of a wall as a simply-supported hinged boundary condition will lead to a conservative solution. Hence, the out-of-plane boundary condition of the inner leaf was treated as a simply-supported system in which the rotations at both the top and the bottom of the wall were not restrained.

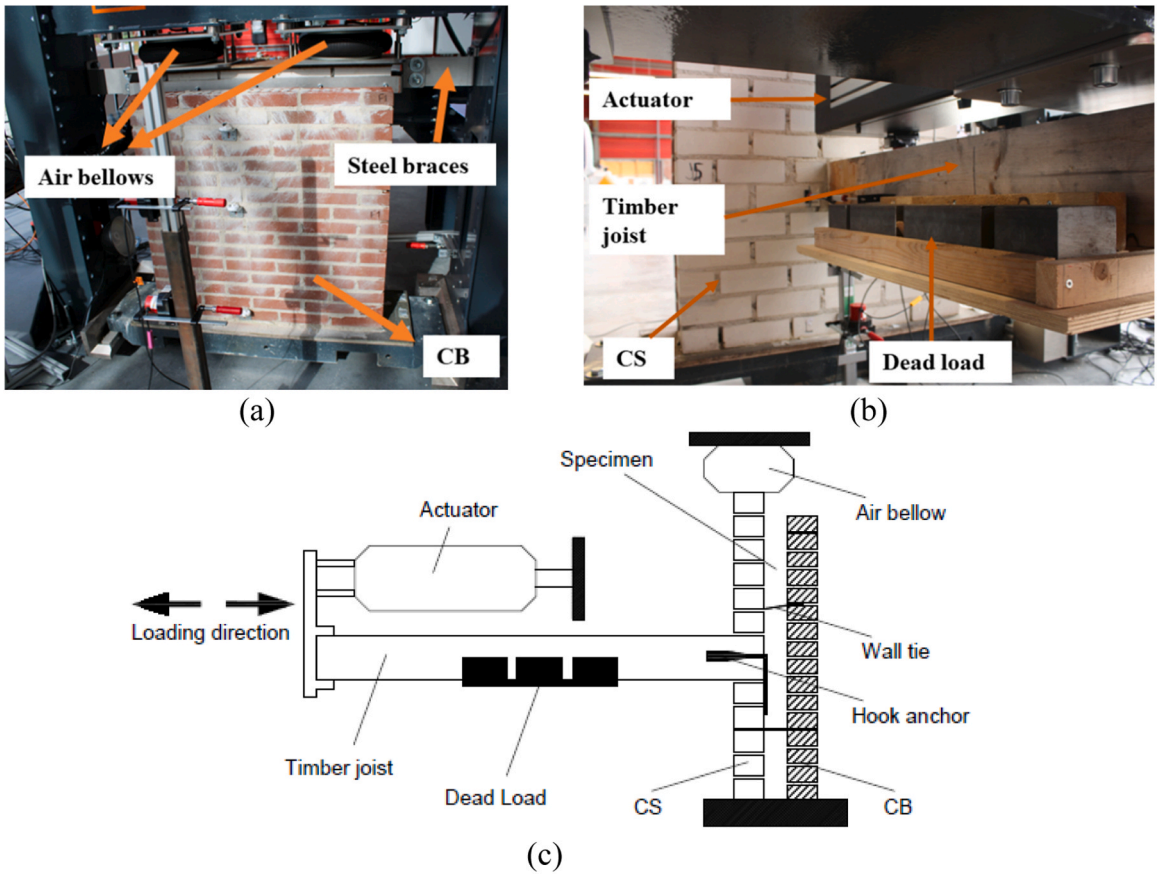

Fig. 4. Test setup: Air bellows, steel plate and braces details (a); detail of actuator and dead load (b) and schematic view of the test setup (c).

The outer veneer was treated as a cantilever system, in which the top edge of the wall was free to rotate and translate. It should be noted that with such a configuration, the equilibrium of the outer leaf is guaranteed by the wall-to-wall connection to the inner leaf. The boundary condition of the specimens is schematically shown in Fig. 5.

The locations of the sensors are illustrated in Fig. 6. The potentiometers were placed symmetrically on both surfaces of the inner and outer leaves to measure the absolute displacement. The relative displacement of the leaves was obtained between the symmetric sensors. The relative displacement between the CS leaf and the joist was measured using potentiometers (7, 8 and 9 in Fig. 6). The absolute displacement of the timber joist was measured by the sensor in the actuator.

2.3. Loading protocol

The specimens were subjected to a quasi-static reversed-cyclic loading to understand better the force-deformation response of wall-to-floor connections, which also closely resemble seismic scenarios [33–35]. Cyclic loading protocols can be found in literature such as European norm EN 12512 [36] or ISO 16670 [37]. In this experimental campaign, the cyclic loading protocol defined according to Method B of the ASTM standard [38] was originally developed for ISO 16670 [37] to be able to compare the findings of this study with those from a previous study [19]. The cyclic protocol was selected with the aim of evaluating the strength and stiffness degradation, as well as the complete hysteretic behaviour of the specimens.

A displacement-controlled procedure was applied. A monotonic test had to be conducted first to determine the ultimate displacement, which was then used as reference deformation to define the amplitudes of the cycles. Hence, the reference deformation of the cyclic test in this study was derived from the monotonic test conducted by Mirra et al. [19], who considered a single-wythe masonry wall with a timber joist with a configuration very similar to that of the present testing campaign. The reference deformation, Δ_m, from the Monotonic tests was chosen equal to a value of 20 mm. The loading protocol consists of three fully reserved cycles at the displacement of 1.25 %, 2.5 %, 5 %, 7.5 %,10 %, 20 %, 40 %, 60 %,80 %, 100 %, 120 %, 140 %, 160 %, 180 %, 200 %, 220 %, 240 % and 280 % of the reference deformation. The loading rate was set at 0.3 mm/s. The cyclic loading protocol is illustrated in Fig. 7.

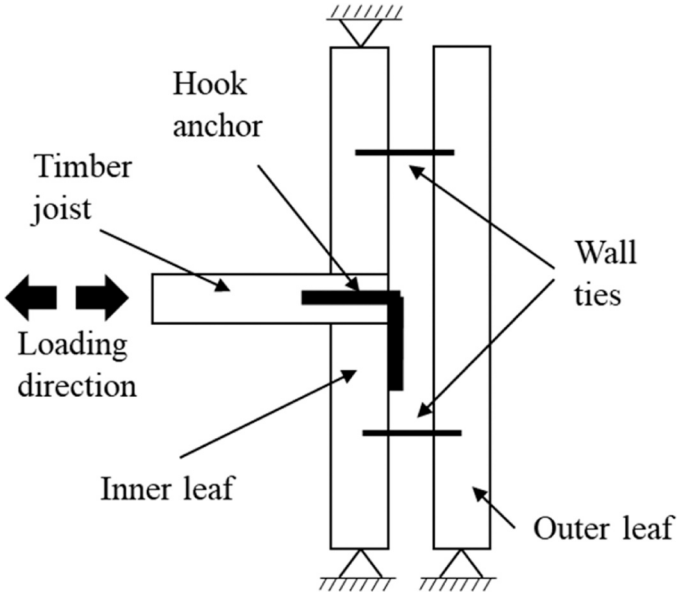

Fig. 5. Schematic of the boundary conditions.

2.4. Mechanical characterisation of the materials

A series of companion tests were performed to characterise the mechanical properties of the materials used in the testing campaign. The flexural and compressive strength of the mortar and the bond strength between the masonry unit and mortar were determined.

The mechanical characterisation of the mortars both for inner and outer leaves was defined in terms of mean compressive strength, f_m, and flexural strength of mortar, f_{bm}, in agreement with NEN-EN 1015–11 [39].

The majority of the masonry buildings in the Netherlands were mainly constructed with low-quality mortar [40]. Hence, both the inner and outer leaves were constructed using a low-strength mortar with a nominal compressive strength of 5 MPa. The results of the flexural and compressive strength tests are reported in Table 2. The flexural tests were performed on 60 specimens and compressive tests on 120 specimens, randomly selected from the batches. The compressive strength was measured equal to 4.25 MPa, whereas the flexural strength to 1.53 MPa. The specimens showed a coefficient of variation approximately equal to 30 % for both tests.

The bond strength between the masonry unit and mortar, f_w, was determined in agreement with the bond wrench test described by EN 1052–5 [41]. Solid clay bricks were used for the outer leaf and CS bricks for the inner leaf. Two types of couplets were tested, representative of the tested specimen in the experimental campaign, namely CS bricks with a low-strength mortar (CS-5 M) and clay bricks with a low-strength mortar (CB–5 M). For each type, a total of 10 couplets were tested for material characterisation. The values of the bond strength of the couplets are shown in Table 3.

Helical bars were used in the retrofitted specimens. Helical bars with a diameter of 6 mm and 304 Grade stainless steel spiral shape were used per each strengthened specimen. A particular material characterisation test for the helical bars used in this experimental campaign was not conducted. However, the properties of the helical bars were taken from the technical description provided by the producer in terms of tensile and compressive strength capacity. The values are summarised in Table 4.

3. Experimental results

This section presents the results obtained in terms of hysteretic behaviour, failure mode, and dissipated energy. The unstrengthened specimens are divided into two categories: mortar pocket connections (Specimens J1, J3 and J5) and hook anchor as-built connections (Specimens J2, J4 and J6). The name of the strengthened specimens (TJ1, TJ2, TJ3, TJ4, TJ5 and TJ6) is obtained by simply adding the prefix T to the corresponding tested unstrengthened specimens. For instance, specimen TJ1 is the strengthened version of the original specimen J1, where helical bars are used for strengthening after the initial tests.

3.1. Hysteretic behaviour

A summary of the peak forces in pulling and pushing, the initial stiffness value and the displacement values at the peak force in pulling and pushing are reported in Table 5. The initial stiffness is determined as the slope of the force-displacement curve up to 1 mm of the relative displacement between the joist and wall. It is important to note that positive displacements and forces correspond to the pulling loading direction of the joist (henceforth called pulling). Hence, the direction of pushing the joist towards the wall (henceforth called pushing) indicates negative forces and displacements.

The hysteretic behaviour of the unstrengthened specimens is reported together with that of the corresponding strengthened specimens in Fig. 8. In addition, a comparison between the as-built and strengthened conditions of each corresponding group in terms of envelope curve

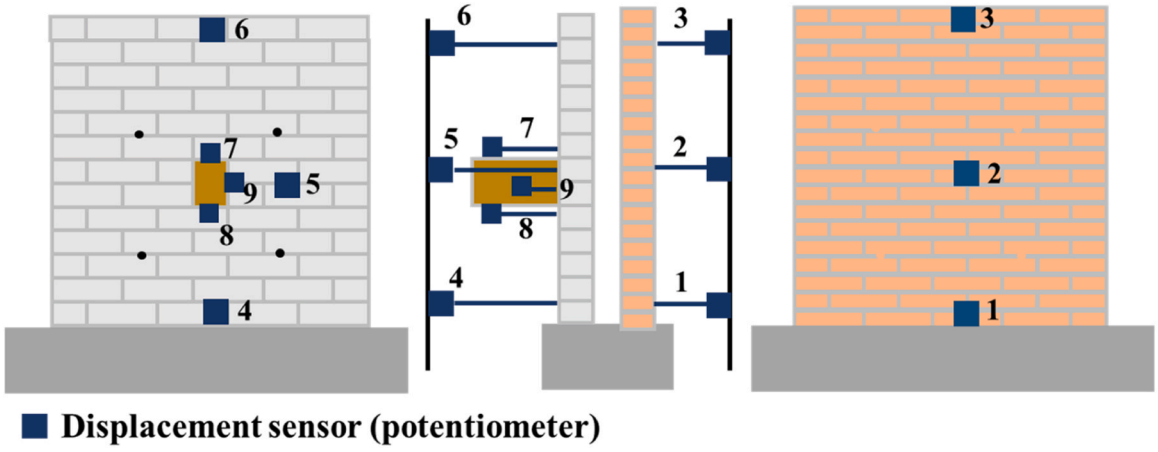

Fig. 6. Location of the sensors.

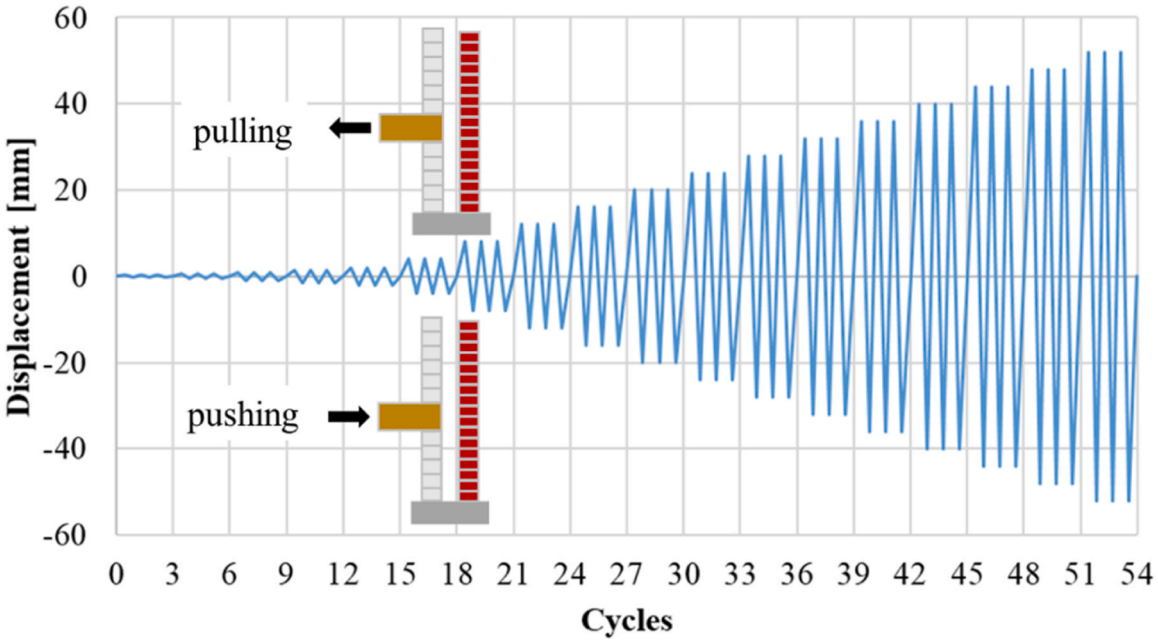

Fig. 7. Cyclic loading protocol.

Table 2
Flexural and compressive strength of CS and CB.

Material property	Symbol	UM	Remix BM2 (5 M)	
			Average	C.oV.
Compressive strength of mortar	f_m	MPa	4.25	0.29
Flexural strength of mortar	f_{bm}	MPa	1.53	0.30

Table 3
Bond strength for each group.

Material property	Symbol	UM	CS - 5 M		CB - 5 M	
			Average	C. oV.	Average	C. oV.
Flexural bond strength	f_w	MPa	0.09	0.15	0.41	0.19

Table 4
Summary of material properties of 6 mm stainless steel spiral Helical bar with 304 Grade.

Loading	Material property	UM	Results from [42]
Tensile loading	0.2 % Proof stress	N/mm^2	995
	Ultimate tensile strength	kN	9.8
	Shear strength	kN	5.5
Compressive loading	Compressive strength (gap=75 mm)	kN	2.20
	Compressive strength (gap=100 mm)	kN	1.59
	Compressive strength (gap=125 mm)	kN	1.15

in pulling and pushing directions is presented in Fig. 8g and h, respectively. The OOP force applied to the wall via the timber joist is plotted against the relative displacement between the joist and the wall.

Regarding the unstrengthened specimens, none of the force-

Table 5
Peak strength in pulling and pushing, initial stiffness and displacement at the peak force in pulling and pushing.

Specimen	Peak force (kN)		Initial stiffness (kN/mm)	Displacement at peak force (mm)	
	Pulling	Pushing	Pulling & Pushing	Pulling	Pushing
J1	2.29	3.13	6.05	0.51	2.15
J2	5.40	1.29	1.20	17.80	48.60
J3	4.02	5.59	15.30	1.32	1.32
J4	4.91	1.59	1.88	19.22	28.13
J5	3.77	4.89	19.49	1.79	3.42
J6	6.63	3.61	2.12	13.36	16.75
TJ1	4.75	4.21	8.80	16.29	1.96
TJ2	6.10	1.44	0.28	20.08	41.38
TJ3	4.05	3.84	3.03	3.75	1.15
TJ4	5.83	4.42	2.11	7.28	3.26
TJ5	5.10	3.36	5.95	7.13	1.05
TJ6	6.07	2.80	2.53	10.54	1.49

displacement curves were perfectly symmetrical with respect to the pulling and pushing directions. The hysteresis loops of the mortar pocket connections (J1, J3 and J5) were mostly characterised by frictional behaviour, but additional contributions due to vertical forces caused by arching actions within the walls were observed, as discussed in detail in Section 3.2. The hysteresis loops of the specimens with hook anchors (J2, J4 and J6) also exhibited highly unsymmetrical behaviour with a pronounced pinching effect, mostly due to the location of the hook anchor, which bares against the exterior surface of the CS leaf in pulling while providing only limited frictional behaviour in the pushing. In pulling, the connection was fully efficient up to high forces, and the joist moved together with the inner leaf. However, when the joist moved toward the wall, the limited friction resistance provided could not limit the relative displacements between the two structural elements.

Given the presence of the additional vertical forces acting on the mortar pocket connections, the values of the peak forces measured for specimens J1, J3, and J5 could not be used to estimate the frictional properties of the connection. However, a relatively symmetric horizontal plateau with elastic-plastic behaviour was observed for the force-displacement curves of these specimens towards the end of the loading protocol. The plastic state was characterised by pure sliding of the joist without any additional contribution. For this reason, the friction coefficient between masonry and timber is computed based on the values of the force at the plastic plateau, averaged for both loading directions. The friction coefficient is therefore estimated equal to 0.6. Such value is deemed appropriate for the contact surface, being in line with the values determined by several studies in the literature [12,13,43]. This value is assumed to be representative of the friction between timber and masonry for every specimen and at any stage of the loading protocol.

Regarding the specimens with timber joist-masonry connections strengthened by means of helical bars, it should be noted that the contribution of cohesion to the capacity of the connection can be neglected since the specimens had already been tested. Nevertheless, the strengthened specimens generally exhibited a higher strength capacity than those in the as-built condition. This is obtained thanks to the capacity of the helical bars to strongly connect the joist to the outer leaf. The failure of the specimens required therefore also the activation of an OOP rocking mechanism of the outer leaf.

A comparison between the performance of Specimens J1 and TJ1 is shown in Fig. 8a. Specimen TJ1 presented higher capacity in both loading directions than that of J1. Additionally, a second peak was observed for Specimen TJ1, larger than the first one, due to the activation of the rocking mechanism of the outer leaf when the full capacity of the cavity wall system was exploited.

Specimens TJ2 performed similarly to J2 (Fig. 8b). In fact, although a strong connection to the outer leaf was achieved at the joist level, which can be detected from the deformation of the outer leaf, the number of cavity wall ties is insufficient to adequately connect the two leaves. Specifically, a horizontal crack developed along the 1st bed joint from the bottom of the outer leaf, followed by the OOP rocking mechanism of the whole cavity wall. However, a second horizontal crack took place in the middle of the CB inner leaf, leading to the instability of this element.

Specimen TJ3 exhibited a more brittle behaviour compared to Specimen TJ1 since the stiffness of TJ3 was higher due to a large number of as-built ties (Fig. 8c). Unlike the previous specimens, horizontal cracks were detected at both the base and the mid-height of the outer leaf in the initial loading stage, thanks to the higher number of ties. The two leaves moved in parallel up to the peak achieved for an imposed displacement of 4 mm, after which the ties partially failed and softening behaviour followed. It is important to point out that the peak force of Specimen J3 was higher than that of J1, which is due to the bond strength. This can be explained by the fact that a stronger bond will not only cause a higher peak force but also a higher arching force while deforming OOP.

Specimen TJ4 showed rocking of the whole system, as described for specimen TJ3, as shown in Fig. 9. In pulling, the post-peak phase was characterised by a plateau up to large displacements (40 mm), similar to the unstrengthened specimen J4, being then the capacity still governed by the effectiveness of the masoned-in anchor (Fig. 8d). On the contrary, in the pushing direction, the post-peak showed a gradual softening behaviour following the development of hinges at the bottom and middle of the outer leaf. Nevertheless, the increase of capacity for the pushing direction compared to that of specimen J4 is noticeable.

Unlike the other specimens, the capacity of the strengthened specimens TJ5 and TJ6 did not reach that of the corresponding unstrengthened specimens, J5 and J6, respectively (Fig. 8e and f). The OOP rocking mechanism of the whole system could not activate because the helical bars ruptured before. This was likely provoked by the larger stiffness and lateral resistance of the wall caused by the higher pre-compression level and the larger number of embedded ties. The behaviour was, hence, governed mainly by the performance of the helical bars, whose asymmetric behaviour in tension and compression also caused the asymmetry of the global hysteresis curve. The helical bars buckled in compression while exhibiting a pull-out failure mechanism in tension.

3.2. *Mechanical contributions to the total connection resistance*

As noted in the previous section, additional vertical forces were introduced at the joist-wallet interface determined by the boundary conditions of the test setup. First, the horizontal top and bottom edges of the specimens were fixed. Hence, when the middle of the wallet was displaced in the OOP direction, the deformation of the specimen and the uplifting resulting from cracking caused an increase in the axial vertical force (due to confinement of the diagonal length of the half wall), as schematically displayed in Fig. 10. This affected the capacity of the connection. It should be noted that this phenomenon is noticeable only when the boundary conditions of the specimen restrict vertical displacements at the top of the wallet; in other words, when the vertical movement of the specimen is either fully or partially restrained. The additional resistance depended on the horizontal bending caused by the displacement imposed at mid-height of the wall. This led to a migration of the neutral axis in the cracked sections and hence introduced an elongation along the centroidal axis and resulted in greater compressive forces. The elongation can be related to the horizontal displacement of the wall at the pocket where the timber joist was inserted through simple geometric observations.

In addition, it should be noted that the joist deflected during the experiment because one extreme of the joist was fixed in the testing machine and could not displace vertically nor rotate, while the other extreme was displaced vertically due to the OOP rocking of the inner leaf and the sliding of the joist in the pocket, as shown in Fig. 11 (the out-of-plane rocking of the wall is amplified to provide a clearer visualization of the vertical displacement). Specifically, the pivot point at the bottom (B in Fig. 11) was assumed to be in the corner of the bottom brick due to

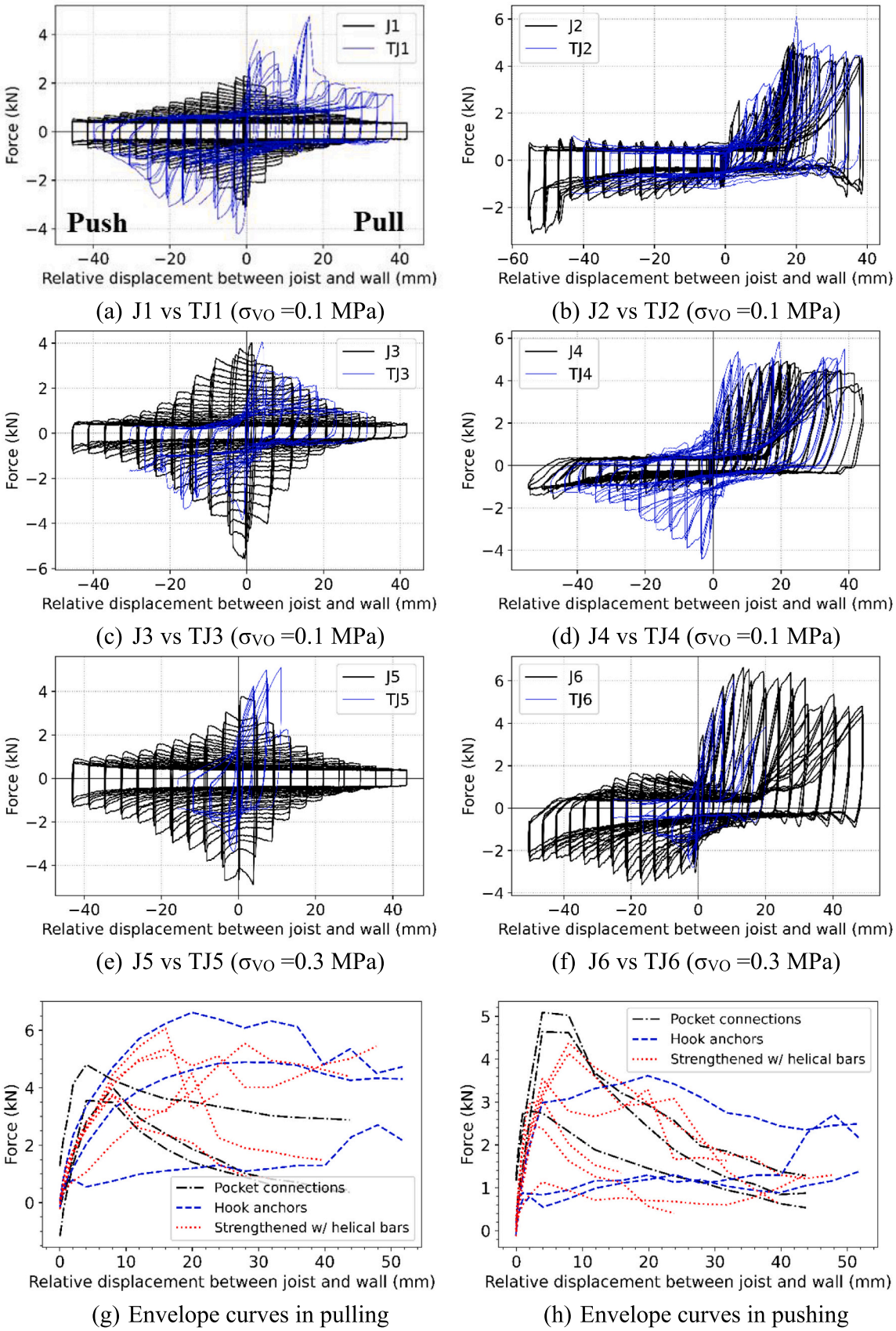

Fig. 8. *Comparison of hysteresis curves of the unstrengthened specimens and the specimens with strengthened timber joist-masonry connection by means of helical bars (mortar pocket connections are shown on the left (a, c, d) and hook anchors on the right of the figures (b, d, f))* as well as envelope curves in terms of in pulling (g) and pushing (h) directions.

Fig. 9. Rocking behaviour of TJ4 under pulling (a) and pushing (b).

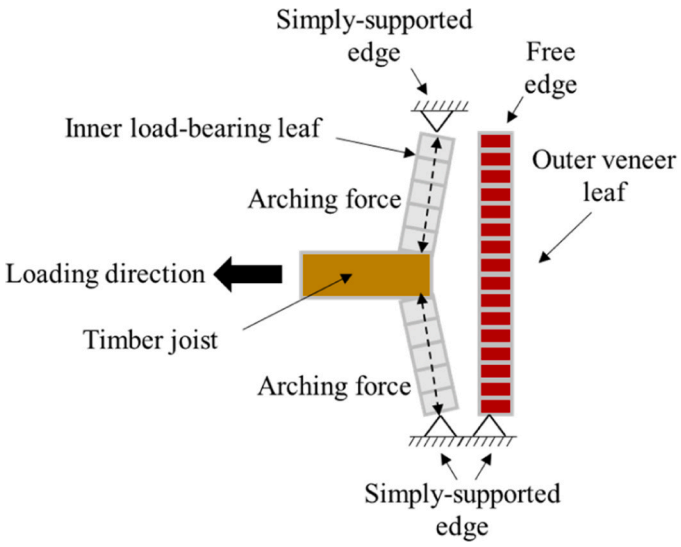

Fig. 10. Schematic description of the arching effect mechanism.

the high rotational stiffness of the support at the base of the wall, while the pivot point at the top (T in Fig. 11) was assumed to be in the middle of the section. Additionally, the sliding can further modify the height of that point. The joist deformation introduced then an additional shear force due to the flexural and shear stiffness of the element.

3.3. Failure mechanisms

In general, the specimens in as-built conditions were tested up to exhibiting moderate damage. Then, the test was stopped, and the specimens were strengthened in order to fully investigate the effectiveness of the retrofitting solution. A review of some observed failure mechanisms is shown in Fig. 12.

The specimens with mortar pocket connections exhibited failure at the joist-wall interface, with a joist-sliding failure mode that included partial joist-to-wall interaction, as explained in Section 3.2. On the other hand, the specimens with hook anchors and the strengthened specimens exhibited a rocking failure mode of the whole system (Fig. 12b and f). Diagonal cracks propagating from the joist were detected (Fig. 12e). Such cracks would not be expected when pure sliding occurs, as observed in the study conducted by Mirra et al. [19]. However, the applied overburden pressure, good initial bond between the joist and the inner leaf, and, especially, the arching effect that developed due to the vertically confined boundary conditions triggered the development and propagation of these cracks.

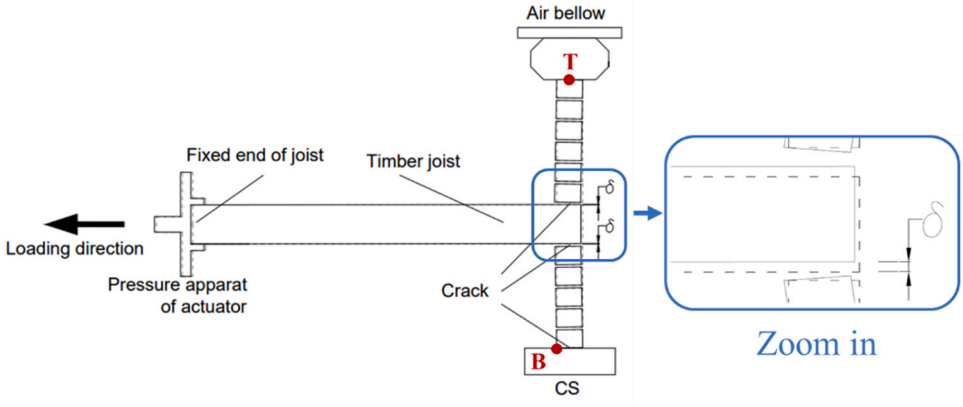

Fig. 11. Vertical deformation of joist at embedded edge during testing.

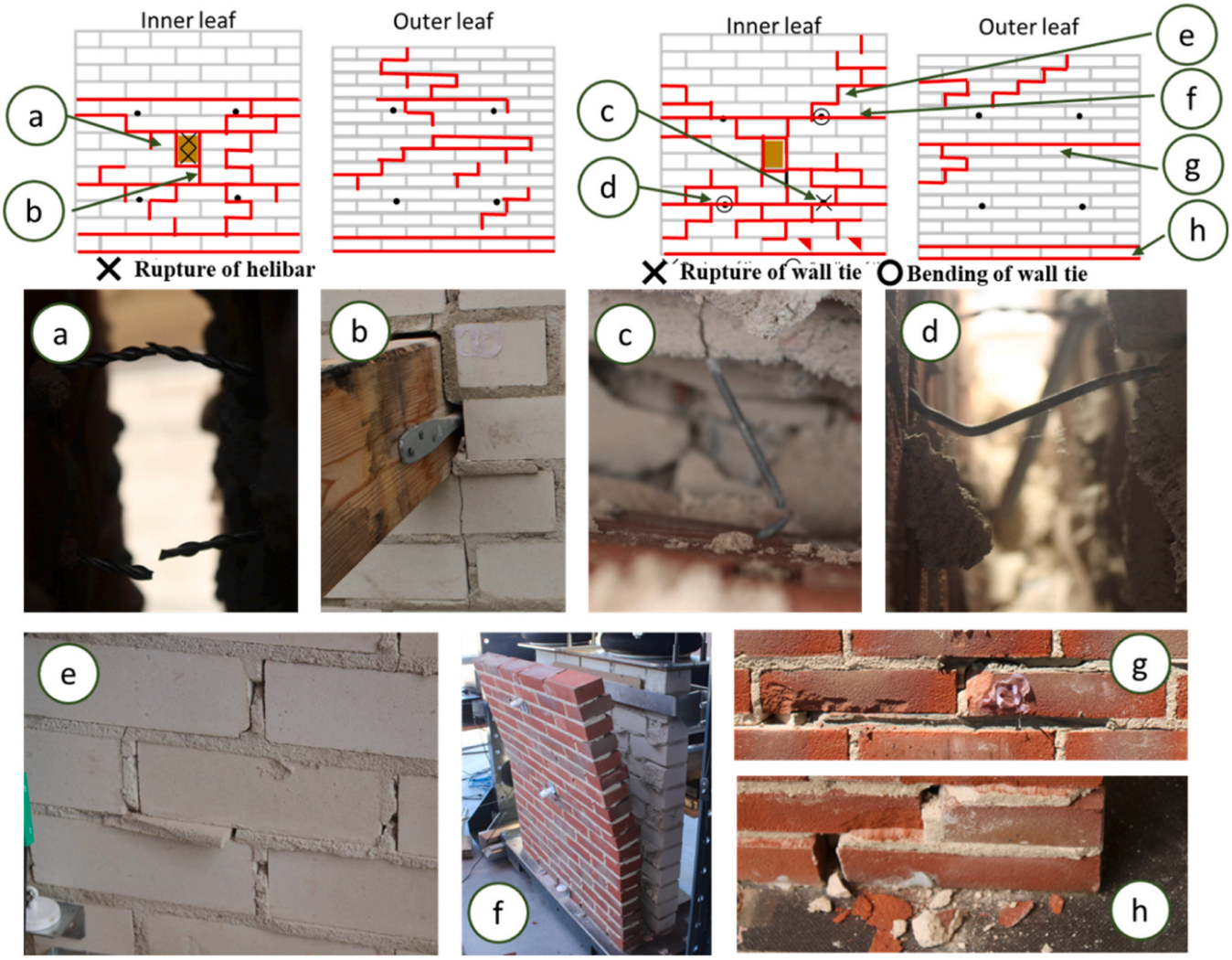

Fig. 12. Observed damage at the end of test Specimen TJ6 and TJ4: Rupture of the helibars (a), sliding of the joist and brick cracking at the location of the hook anchor (b), rupture of the cavity wall tie (c), bending of the wall tie (d), cracks around the embedded wall tie as well as the expulsion of the cone of mortar around the tie (e); OOP rocking mechanism of the outer leaf (f), concentration of damage in the outer leaf due to the helical bars (g), and sliding cracks at the base of the outer leaf (h).

Regarding the specimens with hook anchors, the prevailing failure mode varied depending on the loading direction due to the asymmetric action of the anchors. In the pulling direction, the hook anchor provided a strong bond between the joist and the inner leaf so that an OOP rocking mechanism of the whole system activated and eventually governed the capacity of the specimens. Conversely, in the pushing direction, the anchor did not provide any additional resistance due to the friction between timber and mortar, and a friction-based mechanism governed the failure of the connection. Regarding the strengthened specimens, the rocking failure mode occurred for all the specimens except for specimens TJ5 and TJ6, for which the rupture of the helicoidal bars determined a sudden drop in capacity after the peak load.

To facilitate a better understanding of the failure mode observed for the different specimens, the lateral deformed shape of both inner and outer leaves is plotted in Fig. 13 for the maximum displacements in both positive and negative directions. The deformed shape represents the out-of-plane displacements of the inner and outer leaves measured by the peak displacement in each potentiometer. The displacements of the measured points were then connected by straight lines. It should be noted that the deformations of the unstrengthened specimens from Fig. 13a to Fig. 13f are amplified ten times with respect to real deformations. As expected, the specimens with hook anchors showed higher displacement capacity than that of the specimens with mortar pocket connections, for which the displacement of the joist could not be effectively transferred to the wall (in other words, while the joist displaced, the wall remained almost still). When the unstrengthened and strengthened specimens are compared, the veneer of the strengthened specimens undergoes the rocking-type behaviour, hence exhibiting higher OOP displacement (Fig. 12a, c, and d). This also confirms the contribution of the outer leaves to the resisting mechanism (Fig. 12g and h).

Finally, the effect of the considered variations, namely two different tie distributions, two different pre-compression levels, two different as-built connections, and two different conditions, was evaluated. The main findings are reported as follows:

- The number of as-built cavity wall ties: two vs four (J1 vs J3) – a higher number of as-built ties in the cavity wall contributed to the transfer of the load from the inner to the outer leaf. However, more damage was observed in the inner leaf around the ties. Such damage was observed only in the inner leaf due to the over-resistance of the wall tie embedment in the clay outer leaf with respect to the embedment in the CS inner leaf, as reported in [30].

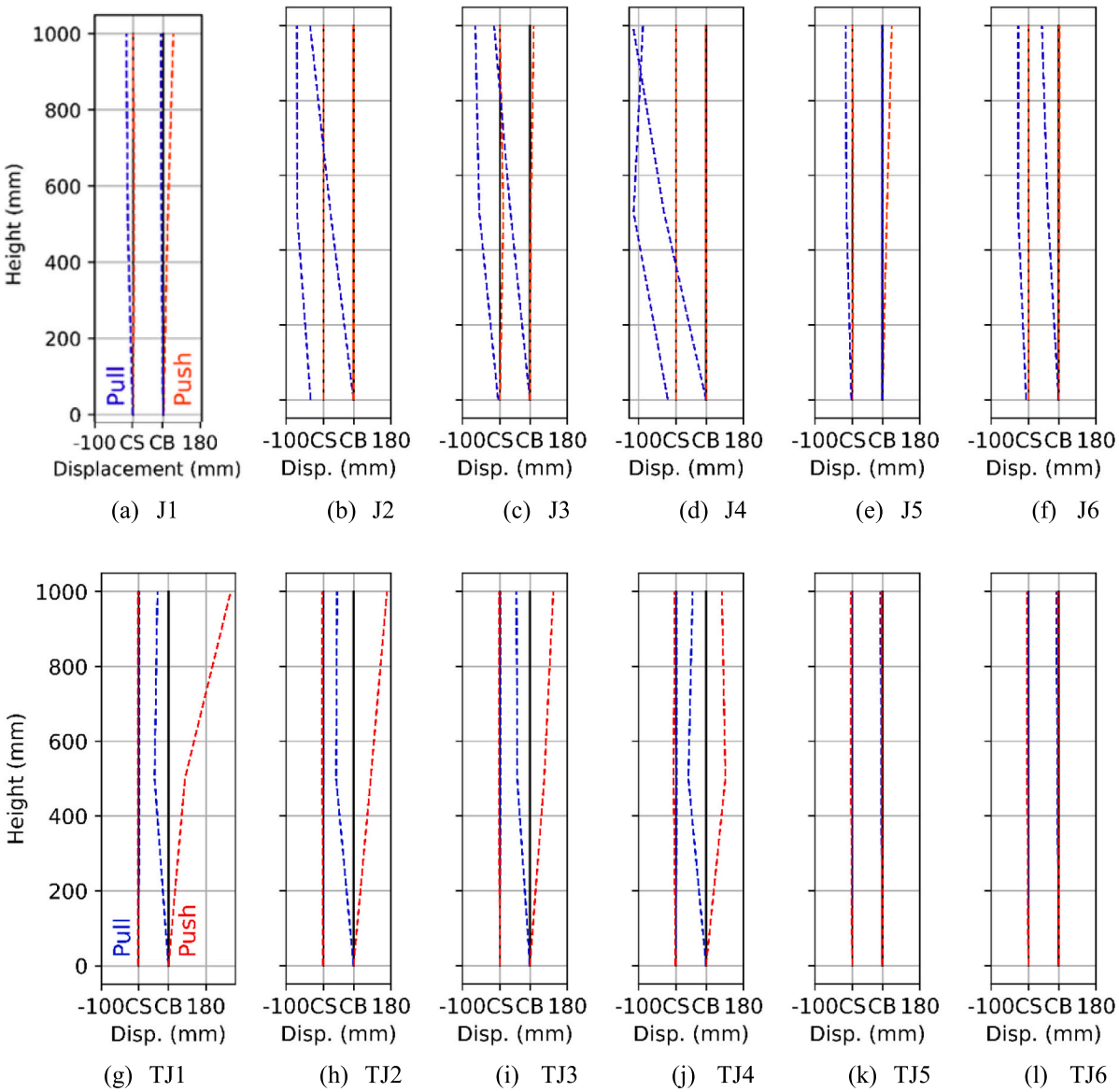

Fig. 13. Deformed shapes of the unstrengthened (from a to f) and strengthened specimens (from g to l). The deformations of the unstrengthened specimens are amplified 10 times with respect to real deformations. The dash lines indicate the out-of-plane displacements of the inner and outer leaves measured by the peak displacement in each potentiometer (the blue dash lines are in pulling, and the red dash lines are in pushing.

- Levels of initial pre-compression: 0.1 MPa vs 0.3 MPa (J1, J2, J3, and J4 vs J5 and J6) – the inner leaf exhibited fewer cracks under higher pre-compression stress conditions. The stiffness of the wall increases with higher overburden.
- Mortar pocket connection vs joist with hook anchor (J1 vs J2) – as extensively discussed in this and in the previous sections, the presence of a hook anchor modifies the failure mode. Specifically, no sliding of the joist was observed in the pulling direction when a hook anchor was installed. On the other hand, this determined more damage in the inner leaf.
- As-built condition vs strengthened condition (J1-J6 vs TJ1-TJ6) – As described above, the strengthened specimens were able to withstand larger deformations related to the rocking response of the system, with the exception of specimens TJ5 and TJ6, whose performance was jeopardised by the rupture of the helicoidal bars.

3.4. Hysteretic energy dissipation

Energy dissipation capacity for connections should be described as an ability to absorb energy input from earthquakes and reduce the amount of energy transmitted to other structural elements. This capacity is a crucial indicator of how well a connection performs under seismic loading. To determine the energy dissipation capacity of the specimens, the cumulative hysteretic energy is calculated based on the area enclosed in the "Force-Displacement" loops. In this case, the force refers to the total reaction force of the joist, while the displacement is the horizontal displacement of the joist. The cumulative hysteretic energy dissipated by the system for a specific displacement of the joist is calculated by adding up the energy dissipated per loop up to that reversed cyclic displacement.

A comparison of the accumulated hysteretic energy for all the specimens is provided in Fig. 14. The as-built specimens with mortar pocket connections dissipated, in general, more energy than those with hook anchors. Such higher dissipation is due to the observed dissipative frictional mechanism. However, specimen J6 dissipated more energy. This is the specimen with a hook anchor and four cavity wall ties, and an applied pre-compression level of 0.3 MPa. The combination of such conditions, which allowed for higher stiffness and resistance, also

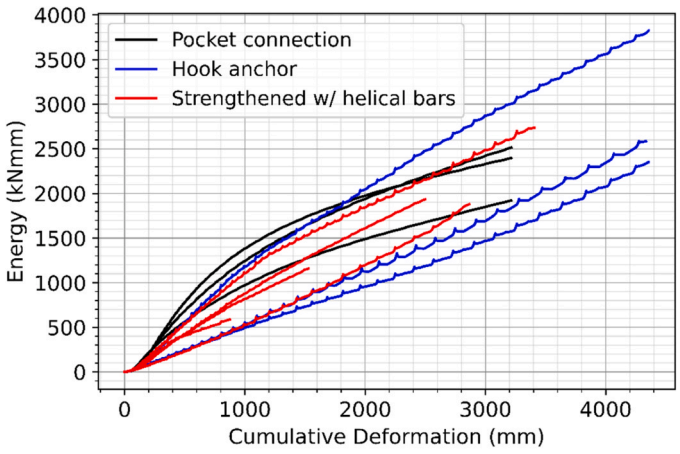

Fig. 14. Comparisons of the specimens with mortar pocket connection, hook anchor and helical bars in terms of cumulative hysteretic energy.

determined more energy dissipation. For the rest of the specimens with hook anchors, the damage localised around the anchor, causing smaller energy dissipation.

Interestingly, the strengthened specimens dissipated a similar amount of energy to those with mortar pocket connections and hook anchors. This is mostly due to the fact that on the one side, the specimens are able to withstand much higher lateral deformations, but on the other side, the rocking mechanism is characterised by low energy dissipation. Additionally, it should be noted that the strengthened specimens lacked initial cohesion, as that was gone during the first testing phase and were already pre-damaged (again, due to the first testing phase) in the surroundings of the connections.

The presented experimental results are based on quasi-static testing, thus certain findings could be different if dynamic earthquake loading was applied. Specifically, the inclusion of inertia and viscoelastic damping in the overall response, as well as the randomness of the loading sequence in the case of dynamic loading via a real accelerogram, could potentially alter the overall response. There is no established difference between dynamic and quasi-static loading cases for masonry; however, some comparative studies in the literature, such as [44], report comparable results for quasi-static and dynamic tests on masonry.

4. Conclusions

This paper presents the findings of an experimental campaign focused on both as-built and strengthened masonry sub-assemblies, specifically those consisting of timber joists connected to cavity walls—the campaign aimed to comprehensively characterise the behaviour of these connections under cyclic axial loading. The results contribute to the existing literature, particularly by comparing as-built and strengthened conditions. Additionally, the findings shed light on the complex interactions between joist and wall-to-wall metal tie connections involving two different wall layers.

Regarding the as-built condition, two different failure modes were observed, depending on the type of connection adopted between the joists and the wall: joist-sliding and rocking failure modes. The joist-sliding failure mode was obtained in case of mortar pocket conditions and also for the specimens with a hook anchor in the pushing direction (i.e., when the joist is pushed closer to the wall). Conversely, the hook anchor provided an adequate bond between the joist and the wall in the pulling direction so that the rocking of the whole system was eventually observed. The capacity of the connection was also affected by an arching effect that was determined by the vertically restrained boundary conditions. On the one hand, this increased the capacity of the connection, but on the other hand, it determined the development of diagonal cracks propagating from the joist in the shape of punching shear.

In the case of specimens with a hook anchor, pinching was observed in the force-displacement curves due to the asymmetric behaviour of the anchor, which bared against the exterior surface of the CS leaf in pulling while providing only limited frictional behaviour in the pushing direction.

For both specimens with a hook anchor and strengthened with helicoidal bars, failure was governed by the out-of-plane rocking of the whole cavity wall system. This behaviour was influenced by the OOP flexural strength of both the inner and outer leaves and by the coupling force provided by the ties between the leaves. In general, only a slight increase in capacity compared to the as-built condition was observed for the strengthened specimens, as an OOP rocking mechanism already limited the capacity of the wall system in as-built conditions. Specifically, an average increase of 10 % in peak load for pulling, while an average decrease of 18 % for pushing was observed. Also, the total hysteretic energy dissipated by the strengthened specimens was comparable to that measured for the as-built ones. The most remarkable benefit of the proposed strengthening solutions was the increased displacement capacity of the system, as well as the limited sliding and possibility unseating of the joist from the pocket.

An increase in the number of wall ties and a higher initial pre-compression level only slightly improved the load capacity of the wall. This limited effect can be attributed to the development of a micro gap around the timber joist interfaces. When the timber joist slid in the pocket back and forth, a micro gap developed around the joist section at the interface between the timber joist and the pocket. Because of the vertical loads on it, the joist was pushed downwards, making stronger contact with the pocket at the bottom face of the connection, while the upper side of the joist remained at a minimal level of contact with the wall. This is the reason why the increased vertical loads on the wall did not significantly increase the vertical stresses at the joist-pocket interface, since they cannot be fully transferred to the joist due to this micro gap at the top of the joist, rendering thus the effects of this increase on the friction resistance of the joist minimal.

The installation of the retrofitting bars not only allowed the system to recover the initial capacity but also ensured deformation compatibility between the wall and joist, thus increasing the overall deformation capacity and ductility of the timber joist-cavity wall system.

It should be noted that the presented tests are quasi-static, while dynamic testing might have provided different results due to the activation of inertia and viscoelastic damping components. Furthermore, a size effect may be inherent in the tests due to the relatively small dimensions of the tested walls as compared to the joist dimensions. Finally, it is important to note that the timber joists in the tested specimens were in ideal perfect conditions, while in reality, such joists may present various imperfections, such as geometric imperfections, excessive moisture and wood decay. Such imperfections may eventually affect the joist response.

Declaration of Competing Interest

The authors declare that they have no known competing financial interests or personal relationships that could have appeared to influence the work reported in this paper.

Acknowledgements

The material adopted in the experimental campaign in the strengthening part for the connection with strengthened timber joists was provided by the company Totalwall. Hence, the authors gratefully acknowledge support from Totalwall and Marten de Jong.

References

[1] Dizhur DY, Moon L, Ingham JM. Observed performance of residential masonry veneer construction in the 2010/2011 Canterbury earthquake sequence. Earthq Spectra 2013;29:1255–74. https://doi.org/10.1193/050912EQS185M.
[2] Arup, Seismic Risk Study - Earthquake Scenario-Based Risk Assessment, 2013.
[3] O. Arslan, Experimental characterisation and mechanical modelling of connection details in traditional Groningen houses, Delft University of Technology, 2023. https://doi.org/10.4233/uuid:6d51ae3a-ffd8–48f1–96ee-89358d3cb5b7.
[4] Dizhur DY, Giaretton M, Ingham JM. URM wall-to-diaphragm and timber joist connection testing. Proc Int Mason Soc Conf 2018;0:1991–2005.
[5] Moshfeghi A, Smyrou E, Arslan O, Bal İE. Out-of-plane shake table tests on solid masonry walls with timber floors. Structures 2024.
[6] J.K. Bothara, R.P. Dhakal, J.B. Mander, Seismic performance of an unreinforced masonry building: An experimental investigation, Earthq. Eng. Struct. Dyn. (2009) n/a-n/a. https://doi.org/10.1002/eqe.932.
[7] Magenes G, Penna A, Senaldi IE, Rota M, Galasco A. Shaking table test of a strengthened full-scale stone masonry building with flexible diaphragms. Int J Archit Herit 2014;8:349–75. https://doi.org/10.1080/15583058.2013.826299.
[8] Magenes G, Penna A, Galasco A. A full-scale shaking table test on a two-storey stone masonry building, 14th. Eur Conf Earthq Eng 2010:384.
[9] Graziotti F, Penna A, Magenes G. A comprehensive in situ and laboratory testing programme supporting seismic risk analysis of URM buildings subjected to induced earthquakes. Bull Earthq Eng 2019;17:4575–99. https://doi.org/10.1007/s10518-018-0478-6.
[10] M. Miglietta, L. Mazzella, L. Grottoli, G. Guerrini, F. Graziotti, Full-scale shaking table test on a Dutch URM cavity-wall terraced-house end unit – EUC-BUILD-6, Res. Rep. EUC160/2018U. (2019).
[11] Kallioras S, Guerrini G, Tomassetti U, Marchesi B, Penna A, Graziotti F, et al. Experimental seismic performance of a full-scale unreinforced clay-masonry building with flexible timber diaphragms. Eng Struct 2018;161:231–49. https://doi.org/10.1016/j.engstruct.2018.02.016.
[12] Almeida JP, Beyer K, Brunner R, Wenk T. Characterization of mortar–timber and timber–timber cyclic friction in timber floor connections of masonry buildings. Mater Struct 2020;53:51. https://doi.org/10.1617/s11527-020-01483-y.
[13] Lin TJ, LaFave JM. Experimental structural behavior of wall-diaphragm connections for older masonry buildings. Constr Build Mater 2012;26:180–9. https://doi.org/10.1016/j.conbuildmat.2011.06.008.
[14] Merriman M. American Civil Engineer's Handbook. New York: John Wiley & Sons, Inc,; 1920.
[15] B. Gigla, Structural design of supplementary injection anchors inside masonry, In: Proceedings of the 15th Int. Brick Block Mason. Conf., Florianópolis, Brazil, 2012.
[16] Porcarelli S, Shedde D, Wang Z, Ingham JM, Giongo I, Dizhur D. Tension and shear anchorage systems for limestone structures. Constr Build Mater 2021;272:121616. https://doi.org/10.1016/j.conbuildmat.2020.121616.
[17] Giuriani E, Gattesco N, Del Piccolo M. Experimental tests on the shear behaviour of dowels connecting concrete slabs to stone masonry walls. Mater Struct 1993;26:293–301. https://doi.org/10.1007/BF02472951.
[18] I. Giongo D. Dizhur R. Tomasi J. Ingham. In-situ testing of wall-to-diaphragm shear transferring connections in an existing clay brick URM building, In: Proceedings of the 9th Int. Mason. Conf. 2014 Guimarães, 2014: pp. 1–12.
[19] Mirra M, Ravenshorst G, de Vries P, Messali F. Experimental characterisation of as-built and retrofitted timber-masonry connections under monotonic, cyclic and dynamic loading. Constr Build Mater 2022;358:129446. https://doi.org/10.1016/j.conbuildmat.2022.129446.
[20] M. Mirra, G.J.P. Ravenshorst, Monotonic, cyclic and dynamic behaviour of timber-masonry connections, 2021.
[21] D. Hoffmeyer B. Rasmussen Housing and construction types country by country - Denmark, DiScript Preimpresion, S. L. 2 2014.
[22] Ingham J, Griffith M. Performance of unreinforced masonry buildings during the 2010 Darfield (Christchurch, Nz) Earthquake. Aust J Struct Eng 2010;11:207–24. https://doi.org/10.1080/13287982.2010.11465067.
[23] Shao J. Sustainable strategies applied on commercial architecture in Australia. Front Archit Res 2013;2:362–72. https://doi.org/10.1016/j.foar.2013.04.005.
[24] Solarino F, Oliveira DV, Giresini L. Wall-to-horizontal diaphragm connections in historical buildings: a state-of-the-art review. Eng Struct 2019;199:109559. https://doi.org/10.1016/j.engstruct.2019.109559.
[25] N. Damiani, M. Miglietta, L. Mazzella, L. Grottoli, G. Guerrini, F. Graziotti, Full-scale shaking table test on a Dutch URM cavity-wall terraced-house end unit – A retrofit solution with strong-backs and OSB boards – EUC-BUILD-7, Pavia, Italy, 2019.
[26] Bruneau M. State-of-the-art report on seismic performance of unreinforced masonry buildings. J Struct Eng 1994;120:230–51. https://doi.org/10.1061/(ASCE)0733-9445(1994)120:1(230).
[27] Giuriani E, Gubana A. A penetration test to evaluate wood decay and its application to the Loggia monument. Mater Struct 1993;26:8–14. https://doi.org/10.1007/BF02472232.
[28] J. Van Den Bulcke, I. De Windt, N. Defoirdt, J. Van Acker, Non-destructive evaluation of wood decay, (2011). www.irg-wp.com.
[29] Macwilliam K, Nunes C. Structural Analysis of Historical Constructions. Cham: Springer International Publishing,; 2019. https://doi.org/10.1007/978-3-319-99441-3.
[30] Arslan O, Messali F, Smyrou E, Bal İE, Rots JG. Experimental characterization of the axial behavior of traditional masonry wall metal tie connections in cavity walls. Constr Build Mater 2021;266:121141. https://doi.org/10.1016/j.conbuildmat.2020.121141.
[31] Graziotti F, Tomassetti U, Penna A, Magenes G. Out-of-plane shaking table tests on URM single leaf and cavity walls. Eng Struct 2016;125:455–70. https://doi.org/10.1016/j.engstruct.2016.07.011.
[32] Morandi P. Second order effects in out-of-plane strength of URM walls subjected to bending and compression. ROSE Sch 2006. https://doi.org/10.13140/RG.2.2.19870.64326.
[33] Giongo I, Dizhur D, Tomasi R, Ingham JM. Field testing of flexible timber diaphragms in an existing vintage URM building. J Struct Eng 2015;141:1–11. https://doi.org/10.1061/(asce)st.1943-541x.0001045.
[34] B.B. Folz, A. Filiatrault, Cyclic analysis of wood shear walls, (2001) 433–441.
[35] Gattesco N, Macorini L. In-plane stiffening techniques with nail plates or CFRP strips for timber floors in historical masonry buildings. Constr Build Mater 2014;58:64–76. https://doi.org/10.1016/j.conbuildmat.2014.02.010.
[36] EN 12512:2001/A1:2005, Timber Structures—Test methods—Cyclic testing of joints made with mechanical fasteners, CEN European Committee for standardization, 2001.
[37] ISO 16670:2003, Timber structures - Joints made with mechanical fasteners - Quasi-static reversed-cyclic test method. International Organization for Standardization (ISO)., 2003.
[38] ASTM E2126–119, Standard test methods for cyclic (reversed) load test for shear resistance of vertical elements of the lateral force resisting systems for buildings., 2019. https://doi.org/10.1520/E2126–19.
[39] Nederlands Normalisatie-instituit (NEN), NEN-EN 1015–11: Methods of test for mortar for masonry - Part 11: Determination of flexural and compressive strength of hardened mortar, (1999).
[40] J. van Elk, D. Doornhof, Material Characterization, 2015.
[41] Nederlands Normalisatie-instituit (NEN), Nen-en 1052–5: Methods of test for masonry - Part 5: Determination of bond strength by the bond wrench method, (2005).
[42] HeliBar, Website of the HeliFix, (2014). http://www.helifix.com/products/retrofit-products/dryfix/.
[43] M. Mirra, G.J.P. Ravenshorst, Seismic characterization of timber-masonry connections based on experimental results, 2019.
[44] ANON.